Finite-Range Calculation of the Two-Neutron Transfer Reaction

B. F. Bayman
School of Physics and Astronomy, University of Minnesota, Minneapolis, Minnesota 55455
(Received 9 November 1970)

Distorted-wave Born-approximation calculations have been done for the reactions $^{40,48}\mathrm{Ca}(t,p)^{42,50}\mathrm{Ca}_{g.s.}$. A finite-range interaction was used, which acted between the proton and each transferred neutron. The results support conclusions of zero-range (t,p) calculations, both with respect to the shapes of the angular distributions, and the relative cross sections for stripping into different shells. However, the calculated absolute cross section is about one third of that observed.

Most distorted-wave Born-approximation (DWBA) analyses of two-nucleon transfer data are based upon the assumption that the transfer process only occurs when the centers of mass of the incoming and outgoing projectiles coincide.[1-4] For example, the (t,p) reaction is treated as if it were due to a zero-range interaction between the proton and the mass center of the transferred neutrons. If, in addition, we neglect spin-flip processes, the differential cross section of a (t,p) reaction with angular momentum transfer L will have the form

$$\frac{d\sigma}{dr} = \Big| \sum_{\substack{n_1 l_1 j_1 \\ n_2 l_2 j_2}} S_{n_1 l_1 j_1, n_2 l_2 j_2}{}^{L} \times F_{n_1 l_1 j_1, n_2 l_2 j_2}{}^{L}(\theta)\Big|^2, \quad (1)$$

in which the $S_{n_1 l_1 j_1, n_2 l_2 j_2}{}^{L}$ are spectroscopic amplitudes, and the functions $F_{n_1 l_1 j_1, n_2 l_2 j_2}{}^{L}(\theta)$ are approximately proportional to each other,

$$F_{n_1 l_1 j_1, n_2 l_2 j_2}{}^{L}(\theta) \approx C_{n_1 l_1 j_1, n_2 l_2 j_2}{}^{L} F^{L}(\theta). \quad (2)$$

The coefficients $C_{n_1 l_1 j_1, n_2 l_2 j_2}{}^{L}$ measure the extent to which the neutrons in the two-neutron state $(n_1 l_1 j_1, n_2 l_2 j_2; L)$ have relative motion similar to the relative motion of the neutrons in the triton. Table I gives the coefficients $C_{nlj,nlj}{}^{0}$ calculated in this way for the $^{40}\mathrm{Ca}(t,p)^{42}\mathrm{Ca}$ ground-state transition, with 10.1-MeV incident tritons. Equations (1) and (2) imply that the relative strengths of transitions with a given L value are determined by the quantities

$$\Big| \sum_{\substack{n_1 l_1 j_1 \\ n_2 l_2 j_2}} S_{n_1 l_1 j_1, n_2 l_2 j_2}{}^{L} C_{n_1 l_1 j_1, n_2 l_2 j_2}{}^{L}\Big|^2. \quad (3)$$

The assumption of a zero-range interaction between the proton and dineutron mass center is made to simplify the numerical calculations. It has not received any physical justification. The problem is complicated by the fact that many of the physically important lengths in the problem have comparable magnitudes (e.g., projectile wavelengths, force range, triton radius, nuclear radius, etc.). Moreover, it is difficult to estimate the normalization of the zero-range interaction, and thus calculations of the absolute cross section are of questionable reliability.

For these reasons, a DWBA calculation for the (t,p) reaction has been performed, in which the interaction has finite range and acts between

Table I. The spectroscopic amplitudes $S_{nlj,nlj}{}^{0}$ for the $^{40}\mathrm{Ca}(t,p)^{42}\mathrm{Ca}$ ground-state transition calculated by Bayman and Hintz, Ref. 3, using a pairing force strength of $20/A$ MeV; the reaction amplitudes $C_{nlj,nlj}{}^{0}$ calculated using the zero-range code TWOPAR; and the $C_{nlj,nlj}{}^{0'}$ determined from the square roots of the factors given in Fig. 2. Both the $C_{nlj,nlj}{}^{0}$ and $C_{nlj,nlj}{}^{0'}$ are normalized to unity for $(2p_{3/2})^2$ transfer.

nlj	$S_{nlj,nlj}{}^{0}$	$C_{nlj,nlj}{}^{0}$	$C_{nlj,nlj}{}^{0'}$
$2s_{1/2}$	−0.09	−0.53	−0.54
$1d_{3/2}$	−0.18	−0.20	−0.22
$1f_{7/2}$	0.97	0.34	0.36
$2p_{3/2}$	0.22	1.0	1.0
$1f_{5/2}$	0.14	0.22	not calculated
$2p_{1/2}$	0.11	0.63	not calculated

the proton and each transferred neutron:

$$V = V(n_1,p) + V(n_2,p), \tag{4a}$$

$$V(n,p) = -[a + b\,\vec{\sigma}_n \cdot \vec{\sigma}_p]\, W(|\vec{n}-\vec{p}|), \tag{4b}$$

$$W(r) = \begin{cases} \infty \text{ if } r \le r_c \\ \exp[-\kappa(r-r_c)] \text{ if } r > r_c. \end{cases} \tag{4c}$$

We have taken $a = 481.21$ MeV, $b = 68.05$ MeV, $r_c = 0.45$ fm, $\kappa = 2.5$ fm^{-1}. This interaction is similar to that used by Tang and Herndon[5] in their variational calculation of the triton wave function (we have used the same range parameter for the singlet and triplet parts of the force, whereas they use a singlet range of 2.211 fm^{-1} and a triplet range of 2.735 fm^{-1}). Our (t,p) calculation also uses the triton wave function calculated by Tang and Herndon. The neutron bound states are calculated in a Woods-Saxon well, whose depth is varied to yield an energy eigenvalue equal to half the two-neutron separation energy. The calculation was restricted to cases with total angular-momentum transfer zero. It involved numerical[6] evaluation of six-dimensional integrals.

The solid line in Fig. 1 shows a semilog plot of the angular distribution calculated in this way for $(2p_{3/2})^2$ transfer onto ^{40}Ca, leading to the ground state of Ca^{42}. The dashed line is the angular distribution for the same transition, but calculated with the zero-range code TWOPAR, which utilizes a modification of the one-particle transfer DWBA code written by W. R. Smith, and a form factor calculated by the method of Bayman and Kallio.[9] The results of this zero-range calculation are arbitrary to the extent of an overall multiplicative factor. This factor is chosen in Fig. 1 to produce closest correspondence between the dashed and solid curves. It is seen from Fig. 1 that the angular distribution calculated from the finite-range expressions has very nearly the same shape as that given by the simpler zero-range code. This similarity was observed in all the calculations performed, for both ^{40}Ca(t,p) and ^{48}Ca(t,p).

Figure 2 shows semilog plots of the angular distributions for transfer of zero-coupled $(2p_{3/2})^2$, $(1f_{7/2})^2$, $(1d_{3/2})^2$, or $(2s_{1/2})^2$ neutrons onto ^{40}Ca, calculated from the finite-range expressions. The scale on the ordinate refers to the solid curve, corresponding to $(2p_{3/2})^2$ transfer. The other curves are scaled by the factors shown in Fig. 2, so as to make the curves coincide in the forward direction. It is seen that the shapes of

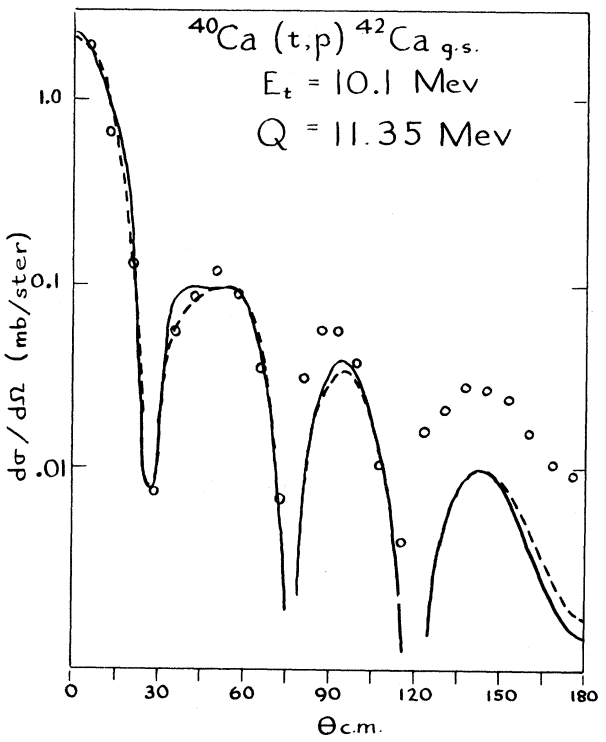

FIG. 1. The solid line shows the angular distribution determined by the calculations reported in this Letter. A pair of zero-coupled $2p_{3/2}$ neutrons is transferred, with $S_{2p_{3/2},2p_{3/2}} = 1$. The optical parameters are the same as those used in Ref. 3. The scale on the ordinate refers to this solid line. The dashed line was calculated with the zero-range code TWOPAR. The circles are the data points of Bjerregaard *et al.*, Ref. 7, multiplied by 0.65 (see Ref. 8).

these four angular distributions are quite similar. This similarity is increased if we compare only the $(2p_{3/2})^2$ and $(1f_{7/2})^2$ curves, or the $(1d_{3/2})^2$ and $(2s_{1/2})^2$ curves. This is expected, because we are then comparing cases in which the neutrons are transferred into the same major shell. Moreover, study of the real and imaginary parts of the reaction amplitudes reveals that these also have angular distributions approximately independent of the shell into which the two neutrons are transferred. Thus the relative cross sections can still be estimated with an expression like (3), the coefficients $C_{nlj,nlj}{}^0$ in (3) being replaced by coefficients $C_{nlj,nlj}{}^{0'}$ given by the square roots of the factors that relate the cross-section curves in Fig. 2. These $C_{nlj,nlj}{}^{0'}$ are also listed in Table I. Comparison of the second and third columns in Table I shows that the zero-range code gives a very good representation of the relative strengths of the $(2p_{3/2})^2$, $(1f_{7/2})^2$, $(1d_{3/2})^2$, and $(2s_{1/2})^2$ transitions.

The sensitivity of the calculated angular dis-

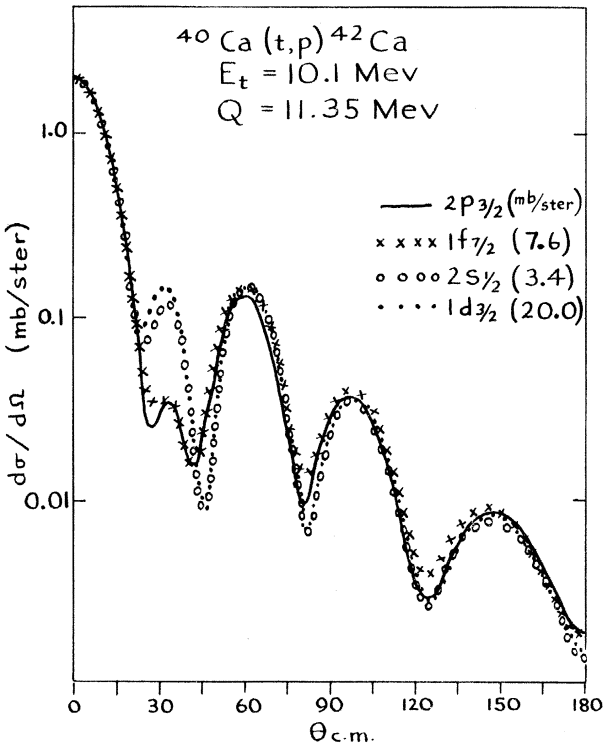

FIG. 2. Comparison of calculated angular distributions for stripping zero-coupled $(2p_{3/2})^2$, $(1f_{7/2})^2$, $(1d_{3/2})^2$, and $(2s_{1/2})^2$ neutrons. The same triton optical parameters were used as for Fig. 1, but the proton parameters were taken from Becchetti and Greenlees, Ref. 10. The scale on the ordinate refers to $(2p_{3/2})^2$ transfer (solid curve). Also listed are the factors by which the other curves had to be multiplied to achieve agreement in the forward direction.

tributions to changes in the optical parameters can be seen by comparing the solid curves in Figs. 1 and 2. These two calculations differ only in their proton optical parameters. It should be noted, however, that although these curves differ in shape, their absolute magnitudes near the diffraction maxima are quite similar. Analogous changes in shape, with approximate preservation of absolute magnitude, were observed when the triton optical parameters were varied.

The first column of Table I shows spectroscopic amplitudes for the ^{40}Ca$(t,p)^{42}$Ca ground-state transition, calculated by Bayman and Hintz[3] from a model in which the neutrons in ^{40}Ca and ^{42}Ca interact via a pairing force of strength $G = 20/A$ MeV. The quantity (3) then has the value 0.54, which implies that the solid line in Fig. 1 should be scaled down by a factor of 0.54 in order to agree with the experimental data. However, to produce the measure of agreement between calculation and data shown in Fig. 1, it was necessary to scale the data down by a factor of 0.65.[8] Thus our calculation underestimates the observed differential cross section by a factor of $0.54 \times 0.65 = 0.35$. The shape of the observed angular distribution is reproduced fairly well by the calculation. A similar estimate for the ^{48}Ca$(t,p)^{50}$Ca ground-state transition shows that our calculated angular distribution is too small by a factor of 0.32.

Our finite-range calculation thus supports the use of zero-range codes for $L = 0$ two-neutron transfers. We concur with their angular distributions, and with their relative cross sections for transferring particles into different shells. However, we have shown that the DWBA treatment, combined with nuclear wave functions containing a reasonable amount of configuration mixing, leads to absolute cross sections that are only about a third of those experimentally observed. This might indicate that the actual transfer mechanism is more complicated than the direct process we assumed, or that there is appreciably more configuration mixing than could arise from a pairing force of reasonable strength. A stronger pairing force ($G = 27/A$ MeV), which overpredicts the odd-even mass difference by about 50%, leads to calculated (t,p) cross sections that are still only about half as large as those observed. It should be borne in mind that these pairing-force calculations include only the six single-particle states near the Fermi surface. Part of the missing (t,p) cross section might be due to the combined effect of many small components in the nuclear wave functions coming from distant configurations.

The author wishes to thank R. A. Broglia for his valuable help throughout the course of this work.

[1]N. K. Glendenning, Annu. Rev. Nucl. Sci. 13, 191 (1963), and Phys. Rev. 137, B102 (1965).

[2]R. M. Drisko and F. Rybicki, Phys. Rev. Lett. 16, 275 (1966).

[3]B. F. Bayman and N. M. Hintz, Phys. Rev. 172, 1113 (1968).

[4]I. S. Towner and J. C. Hardy, to be published.

[5]Y. C. Tang and R. C. Herndon, Phys. Lett. 18, 42 (1965).

[6]The numerical calculations were performed at the Computer Center of the University of Minnesota, and at the Los Alamos Scientific Laboratory.

[7]J. H. Bjerregaard, O. Hansen, O. Nathan, R. Chapman, S. Hinds, and R. Middleton, Nucl. Phys. A103, 33 (1967).

[8]Although the shape of the angular distribution was measured with 10.1-MeV tritons, the magnitude of the cross section was measured with 12-MeV tritons. Estimates with our zero-range code indicate that the effect of this 2-MeV energy difference on the magnitude of the cross section should be less than 7%.

[9]B. F. Bayman and A. Kallio, Phys. Rev. 156, 1121 (1967).

[10]F. D. Becchetti, Jr., and G. W. Greenlees, Phys. Rev. 182, 1190 (1969).

Formation of Geons and Black Holes

Ulrich H. Gerlach*
Battelle Memorial Institute, Columbus, Ohio 43201
(Received 21 September 1970)

We determine the dynamics of a spherically symmetric, thin-shelled ensemble of collisionless particles. All the stable and unstable equilibrium configurations (which we find to be stable against single-particle decay) are classified with the help of a variational principle. Applying this principle to zero-rest-mass particles (e.g., gravitational geon), we find that quantum geometrodynamics must be applied when the geon has low angular momentum and is in its ground state.

The hydrodynamics of spherically symmetric gravitational collapse[1] has advanced to the stage where, in order to gain new knowledge, one must merely solve the appropriate equations for the particular situation under study. Because of their nonlinearity, some very interesting information can be extracted from these equations only with great financial efforts: Involved computer calculations are necessary to solve the equations.[2]

Consequently, our work has been to set up and solve analytically an archetypical model for gravitational collapse[3,4]: Although this model ignores the detailed internal, hydrodynamic features, it incorporates those essential features that determine whether or not a black hole or a geon is formed. Consider a spherically symmetric ensemble of noncolliding particles (with or without rest mass), each having a given angular momentum l. The stress-energy tensor and the particle flux vector are[5]

$$T_\nu{}^\mu = \int N p_\nu p^\mu d\omega,$$
$$J^\mu = \int N p^\mu d\omega,$$

respectively. Here N is the invariant single-particle distribution function that satisfies the Liouville equation, p^μ is the particle four-momentum, and $d\omega$ is the invariant three-momentum volume element.

We shall selectively focus on ensembles that are hollow thin-shelled spheres. Within a shell the particles are churning back and forth within a small energy range. Consequently, an observer moving with the thin shell notices that

$$T_0{}^0 = c p_0 J^0, \tag{1}$$

where c is the speed of light.

First we wish to determine the equilibrium configurations of the particle ensemble. Consequently, we focus attention on all the momentarily static configurations. The conservation of particle number and the initial-value equations of general relativity yield

$$da/dR = 4\pi R^2 J^0 \exp[\tfrac{1}{2}(\lambda+\nu)] \tag{2}$$

and

$$dm/dR = -4\pi R^2 T_0{}^0 \tag{3}$$

in the Schwarzschild coordinates,

$$ds^2 = -e^\nu dt^2 + e^\lambda dR^2 (d\theta^2 + \sin^2\theta d\varphi^2). \tag{4}$$

Here a and m are the particle number and the mass enclosed by a sphere of radius R. The radial metric coefficient is given by[6]

$$e^\lambda = (1-2m^*/R)^{-1},$$

and the energy of the particles is peaked around

$$-c p_0 e^{-\nu/2} = c(l^2/R^2 + \mu^2 c^2)^{1/2}, \tag{5}$$

where l is the conserved angular momentum and μ is the rest mass of each particle. For momentarily static particle ensembles, having total particle number A, the total mass energy as seen by a distant observer is determined from the differential equation

$$\frac{dm^*}{da} = \left(1-\frac{2m^*}{R}\right)^{1/2}\left(\frac{l^2}{R^2}+\mu^2c^2\right)^{1/2}\frac{G}{c^3}. \tag{6}$$

This equation is the consequence of dividing Eq. (2) into Eq. (3) and then making the appropriate substitutions for $e^{\lambda/2}$, $T_0{}^0$, and $p_0 e^{-\nu/2}$. Integrat-